Proceedings of *RAGtime 10–13, 15–17/20–22/15–17/14–16 September, 2008/2009/2010/2011, Opava, Czech Republic*
Z. Stuchlík, G. Török and T. Pecháček, editors, Silesian University in Opava, 2014, pp. 209–229

Modelling steep radial emissivity in relativistic iron lines from black-hole accretion discs

Jiří Svoboda[1,2,a], Michal Dovčiak[1], Vladimír Karas[1] and René Goosmann[3]

[1]Astronomical Institute, Academy of Sciences, Boční II. 1401, CZ-141 31 Prague, Czech Republic
[2]European Space Astronomy Centre of ESA, Spain
[3]Strasbourg Observatory, France
[a]jiri.svoboda@asu.cas.cz

ABSTRACT
X-ray spectroscopy of active galaxies and black hole binaries provides an opportunity to explore the innermost regions of black hole accretion discs. Some of the recent measurements have revealed a very steep radial decrease of the disc reflection emissivity, especially in the central region, suggesting the disc-irradiating corona to be compact and very centrally localised. We discuss whether the special conditions on the corona properties are indeed required, and / or whether the steep radial emissivity could be an artefact of model assumptions. The inter-dependencies and possible degeneracies between the radial emissivity index and other parameters of the relativistic reflection model are studied. A set of simulations using a preliminary response matrix for a planned Athena mission is performed for this purpose. We show that the measurements of the radial emissivity are indeed degenerate with some model assumptions and parameters, even for more sensitive spectra than for those available from current X-ray missions. We also realise that the radial dependence of the disc ionisation might be another factor which can account for the steep radial emissivities.

Keywords: black holes – accretion discs – relativistic iron lines

1 INTRODUCTION

Relativistic iron lines in X-ray spectra of active galactic nuclei and black hole binaries represent one of the most suitable opportunities to measure the angular momentum of accreting black holes, see e.g. Reynolds and Nowak (2003) for a review. Spin measurements are influenced by the geometry of the disc-illuminating corona and local properties of the disc that affect the re-processing and re-emission of the incident photon. Usually, the current iron line models (Laor, 1991; Dovčiak et al., 2004; Beckwith and Done, 2004; Brenneman and Reynolds, 2006) employ a simplified approach where the complex relationship between

978-80-7510-125-9 © 2014 – SU in Opava. All rights reserved.

the disc illumination and consequent emission is approximated by a simple or broken power-law dependence on radial coordinate, and local angular emissivity profile is assumed to be either isotropic or limb-darkened.

In our recent paper (Svoboda et al., 2009), we investigated the effect of different emission angular directionality on the spin measurements. Here, we extend our analysis by study of a possible degeneracy between the assumption of the angular distribution and model parameters describing the radial profile of the emissivity. More generally, we investigate further effects which might account for the radial emissivity profile, namely the localisation of the corona and the radial structure of the disc ionisation.

The intrinsic disc emissivity is naturally expected to decrease with the growing distance. The temperature of the disc decreases as r^{-3} (Shakura and Sunyaev, 1973; Novikov and Thorne, 1973). Therefore, one of the naive assumptions is to assume the same dependence for the reflection, i.e. the reflection emissivity $\epsilon \propto r^{-q}$, where $q = 3$. The simplest physical picture is that of a corona uniformly sandwiching the disc. The more energetic photons are injected in the innermost regions, and so, more intense irradiation of the disc occurs there.

However, non-thermal coronal emission does not necessarily need to behave in the same way as the thermal dissipation of the disc. The interaction between the disc and the corona is more complicated, including the radiation and magnetic processes (see e.g. Haardt and Maraschi, 1991; Czerny and Goosmann, 2004; Goosmann et al., 2006; Różańska et al., 2011). Especially when the magnetic field is considered, the resulting profile might be as steep as e.g. r^{-5} (Kawanaka et al., 2005).

Steep radial emissivities were indeed reported in several sources, in active galaxies like MCG -6-30-15 (Fabian et al., 2002; Vaughan and Fabian, 2004; Miniutti et al., 2007), 1H0707-495 (Fabian et al., 2009; Zoghbi et al., 2010; Dauser et al., 2012), IRAS 13224-3809 (Ponti et al., 2010) as well as in black hole binaries, e.g. XTE J1650-500, GX 339-4 (Miller, 2007). In order to provide a physical picture of the steep radial emissivity in MCG -6-30-15, Wilms et al. (2001) invoke strong magnetic stresses that should act in the innermost region of the system. This should correspond to the enhanced dissipation of a considerable amount of energy in the accretion disc at small radii. If the magnetic field lines thread the black hole horizon, the dissipation could be triggered by magnetic extraction of the black hole rotational energy, perhaps via Blandford–Znajek effect (Blandford and Znajek, 1977), but it could be also supplemented by a rather efficient slowing of the rotation, as also seen in recent GRMHD simulations (e.g. Penna et al., 2010). The efficiency of the competing processes still needs to be assessed.

Martocchia et al. (2000) examined whether the required steep emissivity law as well as the predicted equivalent width of the cold reflection line of iron and the Compton reflection component can be reproduced in a phenomenological (lamp-post) model where the X-ray illuminating source is located on the common symmetry axis of the black hole and the equatorial accretion disc. These works suggested that the radial emissivity function of the reflection component steepens when the height parameter of the primary irradiation source decreases. The enhanced anisotropy of the primary X-rays was identified as a likely agent acting in this process. The emissivity in the XMM-Newton spectrum of MCG -6-30-15 was successfully reproduced with the lamp-post geometry (Martocchia et al., 2002; Miniutti et al., 2003).

In some cases, like in the spectrum of 1H0707-495, the measured radial emissivity in the innermost region $q \approx 7$ (Fabian et al., 2009; Wilkins and Fabian, 2011) is, however, steeper than any current theoretical model predicts. In this paper, we will discuss some possible explanations of detecting such steep radial emissivities. To this end, we explore several simple test models and analyse them with the simulated data.

2 DATA SIMULATION

We used a preliminary response matrix[1] for the planned X-ray mission Athena (Nandra, 2011) in our various simulations. There are several reasons for this choice. First of all, this mission has been proposed only recently and ongoing scientific discussions on feasible applications are timely. We would like to show by this analysis that in the case of approval the Athena mission will be suitable for studying reflection features from the innermost accretion discs around black holes. The main aim of these simulations is to constrain possible degeneracies among different parameters of the relativistic reflection model. For this purpose, Athena allows for a more sensitive analysis than is possible with the spectra from current X-ray missions. Using a sensitive response planned for the future mission allows us to find degeneracies which are not only adherent to the current data, but which also will not be resolved with the on-coming X-ray detectors.

We performed the spectral analysis between 2–10 keV energy range where one of the most prominent reflection feature, the iron Kα line, occurs. We re-binned the response matrix by a factor of 10 between channels 2700 and 8800 (2–10 keV), the other channels were not used. We used Xspec (Arnaud, 1996), version 12.6.0ab for the spectral fitting. We used the most recent version of KY code (Dovčiak et al., 2004) which includes the lamp-post geometry (Dovčiak et al., in prep.). The flux of the model was chosen to be similar to that of bright Seyfert galaxies, i.e. $\approx 3 \times 10^{-11}$ ergs·cm^{-2} s^{-1} (Nandra et al., 2007). The simulated observation time was always 100 ks, which is a typical value for average exposure time of AGN observed with the current X-ray satellites.

3 LAMP-POST SCHEME

First, we investigate how the radial emissivity depends on the geometry of the corona. If the corona is localised the illumination of the disc decreases with the growing distance from the source in a particular way determined by the position of the corona and by the gravitational pull of the central black hole. The configuration when the corona is very compact and located just above the black hole, known also as the lamp-post scheme, has been studied as a simple disc-corona scenario by Matt et al. (1991); George and Fabian (1991). In a physical picture, the source above the black hole can be imagined, e.g. as a base of a jet.

In this scenario the irradiation far from the source radially decreases as r^{-3}. In the central region, the relativistic effects – energy shift, aberration and light-bending – influence the disc illumination, and thus shape the reflection spectra of black hole accretion discs (Miniutti and Fabian, 2004). As a result, the different parts of the disc are irradiated with different

[1] up-to-date to 9/5/2011, ftp://ftp.rssd.esa.int/pub/athena/09052011_Responses

Table 1. The inner radial emissivity index $q_{\rm in}$, and the break radius $r_{\rm b}$ inferred for different heights and directionalities in the lamp-post model.

$a = 0.94$

	numerical		limb brightening		isotropic		limb darkening	
$h[r_g]$	$q_{\rm in}$	$r_{\rm b}$	$q_{\rm in}$	$r_{\rm b}$	$q_{\rm in}$	$r_{\rm b}$	$q_{\rm in}$	$r_{\rm b}$
1.5	$4.8^{+0.2}_{-0.1}$	$6.1^{+0.2}_{-0.2}$	$4.5^{+0.1}_{-0.1}$	$6.4^{+0.2}_{-0.2}$	$5.0^{+0.4}_{-0.1}$	$6.0^{+0.3}_{-0.2}$	$5.3^{+0.1}_{-0.1}$	$5.7^{+0.2}_{-0.1}$
3.0	$3.3^{+0.1}_{-0.1}$	$6.3^{+1.9}_{-1.1}$	$3.2^{+0.3}_{-0.2}$	$8.0^{+3.4}_{-2.6}$	$3.2^{+0.1}_{-0.1}$	15^{+10}_{-3}	$3.3^{+0.1}_{-0.1}$	20^{+70}_{-5}
10	$1.3^{+0.1}_{-0.2}$	16^{+1}_{-1}	$2.3^{+0.1}_{-0.1}$	55^{+9}_{-10}	$2.3^{+0.2}_{-0.1}$	48^{+5}_{-7}	$2.5^{+0.1}_{-0.1}$	60^{+15}_{-15}

intensity, making the emissivity profile in reflection models distinct from the standard value of $q = 3$. If the height of the source is sufficiently close to the black hole event horizon the light bending implies higher irradiation of the innermost region compared to the outer parts of the disc. In the most extreme scenario, when the source is moving towards the black hole, the Doppler boosting might increase this effect. However, there is no observational evidence for such an inflow of the matter perpendicular to the disc plane, while outflows in the form of a jet are observed in many sources (e.g. Merloni et al., 2003).

Further, we consider the stationary lamp-post source and investigate the radial emissivity profile of the disc reflection radiation for different heights of the source. The fully relativistic code including the azimuthal dependence of the reflected emission coming from a neutral disc was employed. The radial emissivity profiles are shown in Dovčiak et al. (in prep.). Here, we study whether it is possible to approximate the radial emissivity in the lamp-post model by a simplified profile in the form of a broken power-law, as this is usually used in current modelling of the data.

Figures 1 and 2 show contour plots for the radial emissivity index and the spin, and the break radius, respectively. The fiducial value of the spin was set to $a = 0.94$ (indicated by the dashed line). The other parameters of the seed model were the photon index of the primary power-law radiation $\Gamma = 1.9$, the inclination of the disc $i = 30\,$deg, the inner radius $r_{\rm in} = r_{\rm ms}$, and the outer radius $r_{\rm out} = 400\,r_{\rm g}$. The data were modelled by the power-law component with the fixed value of the photon index and the KYRLINE model for the iron line with the adopted broken power-law for the radial emissivity. Different angular directionality was used (see the next section for further details). The best-fit parameters are summarised in Table 1. In the contour calculations, only the two interesting parameters were allowed to vary. Others were fixed to their default or best-fit (in the case of break radius) values.

Figures 6–8 show the same but for different parameters. The steep radial emissivity is reached only if the primary source is at a very low height above the black hole where the strong gravity considerably bends the light rays of the primary radiation. Very steep radial emissivities detected in the spectra would imply that the black hole must be rapidly rotating, and moreover, the source would have to be very bright because the radiation would lose its intensity on its way out of the deep gravitational well.

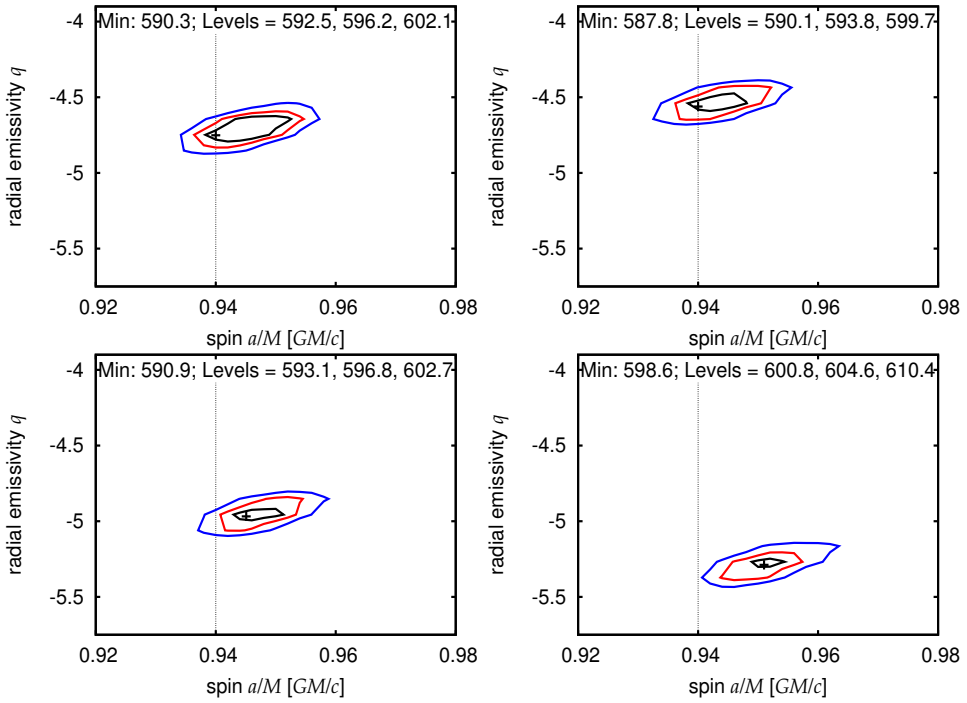

Figure 1. Contour plots of the spin a and the radial emissivity parameter q. The data were generated with the lamp-post model with the height $h = 1.5\,r_{\rm g}$. The default value of the spin was $a = 0.94$, which is indicated by a dashed line in the graph. Different prescriptions for the angular emissivity were used: *Top left:* angular emissivity from numerical calculations. *Top right:* limb brightening. *Bottom left:* isotropic. *Bottom right:* limb darkening. The χ^2 values corresponding to the best fit (minimum) and to the 1σ, 2σ, 3σ levels are indicated in the text legend.

4 INTERPLAY BETWEEN THE RADIAL AND ANGULAR EMISSIVITY PROFILE

When fitting the data, the local intensity of the re-processed radiation emitted from the disc is often assumed to be divided into two separate parts – the radial and angular dependence. The latter one characterises the emission directionality. However, due to large rotational velocity of the disc and the strong gravity near the black hole, the photons that reach the observer are emitted under different angles at different locations. Therefore, the angular part of the emissivity depends on radius as well, and the above separation is not valid. The relativistic effects, aberration and light bending, cause that the emission angle in the innermost region is always very high (almost 90 degrees with respect to the disc normal) – see Appendix C in Dovciak (2004), or Fig. 3 in Svoboda et al. (2009). Although it is not an axi-symmetric problem, the almost radial decrease of the emission angle is apparent, which invokes the link between the radial and angular emissivity (Beckwith and Done, 2004; Svoboda et al., 2009).

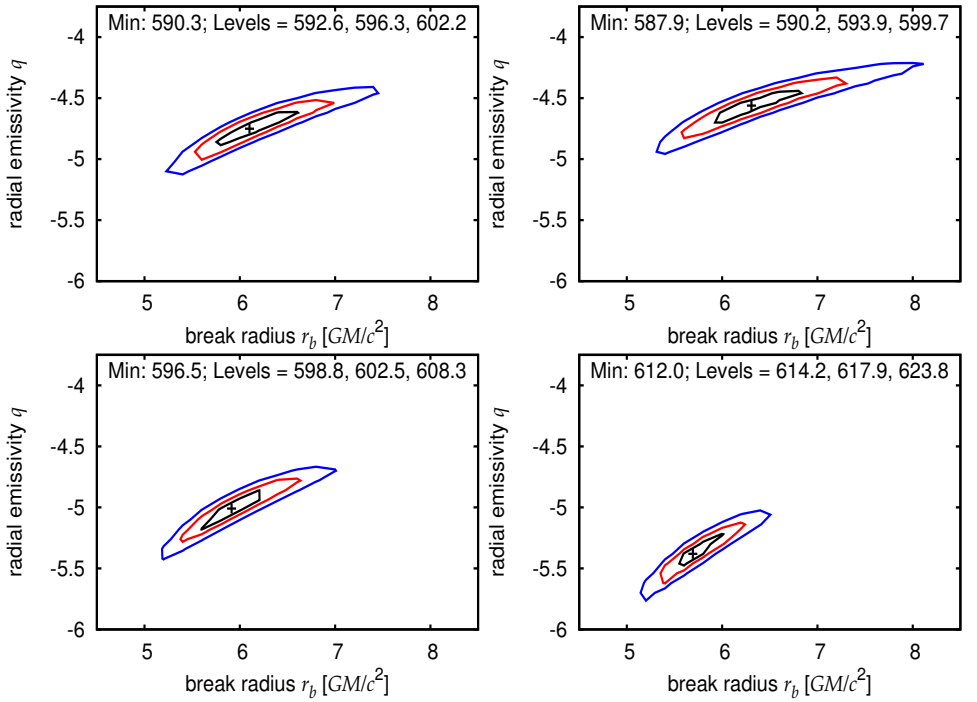

Figure 2. Contour plots of the radial emissivity and the break radius for the height $h = 1.5\,r_{\rm g}$. The legend is the same as in Fig. 1. The spin and the inclination were frozen to their default values.

Hence, we used different assumptions about the directionality:

(1) our numerical computations[2] (Svoboda et al., 2009),
(2) limb brightening $I(\mu_{\rm e}) \approx \ln(1+\mu_{\rm e}^{-1})$ (Haardt, 1993),
(3) isotropic,
(4) limb darkening $I(\mu_{\rm e}) \approx 1 + 2.06\mu_{\rm e}$ (Laor, 1991),

where $\mu_{\rm e}$ is the cosine of the emission angle. The simulated data were created with our numerical model of the directionality calculated with the NOAR code (Dumont et al., 2000). Free-free absorption, the recombination continua of hydrogen- and helium- like ions, the direct and inverse Compton scattering were taken into account (see Svoboda et al., 2009, for more details).

The fact that we get different results confirms that constraining the radial emissivity is influenced by the prescription for the angular emissivity. Steeper radial emissivities are required in the best fits with limb darkening. This emissivity law is widely used in the reflection models, however, it is somewhat in contradiction with several models of X-ray illuminated disc atmospheres (Ghisellini et al., 1994; Zycki and Czerny, 1994; Goosmann

[2] integrated over incident angles

et al., 2006; Różańska et al., 2011). Its application causes an appreciable underestimation of the innermost flux. The radial emissivity parameter must then be set to an artificially steeper value in order to compensate this loss of the counts from the central region where the emission angle is grazing.

5 RADIALLY STRUCTURED IONISATION OF THE DISC

The interplay between the radial and angular emissivity shows that the steep radial emissivity in the observational data might be caused by an invalid model assumption. Yet, there is another frequently used assumption in the reflection scenario that can contribute to this effect as well – the constant ionisation over the whole surface of the disc. The intensity of the disc irradiation, whether it is approximated by a (broken) power-law decrease or by a lamp-post illumination in curved space-time, decreases with the radius. Therefore the ionisation of the disc surface may respond accordingly, as suggested before by Matt et al. (1993).

Ballantyne et al. (2001) investigated the importance of the photo-ionisation of the disc surface in active galactic nuclei. The presence of ionised reflection features in their X-ray spectra was reported in several sources (see Ballantyne et al., 2011, and references therein). The photo-ionisation was also suggested as a possible explanation for non-detection of the spectral imprints of the relativistically smeared reflection (Reynolds et al., 2004; Svoboda et al., 2010; Bhayani and Nandra, 2011; Brenneman et al., 2012). The radially dependent ionisation was discussed recently with the existing data by Zhou et al. (2011).

More generally, the ionisation of the disc surface depends on several other physical quantities like density, vertical structure, thermal heating etc. (see e.g. Nayakshin and Kallman, 2001; Różańska et al., 2002; Goosmann et al., 2007 and references therein). A detailed description of the disc ionisation is beyond the scope of this paper. Here, we simply suppose that the radial dependence of the ionisation may be relevant, as a natural consequence of the radial dependence of the disc illumination by the primary radiation. Thus, we suppose that the accretion disc around a black hole might be more ionised in the central region and colder in the outer regions.

5.1 Test case: two ionisation zones

Currently, no model can consistently describe the radial structure of the disc ionisation. Hence, as a test case, we used two REFLIONX models (Ross and Fabian, 2005) with a different ionisation state convolved with KY model (Dovčiak et al., 2004), corresponding to different emission regions on the disc. The inner disc ionisation was set to $\xi = 50, 80, 100, 130, 150, 200\,\mathrm{ergs{\cdot}cm\,s^{-1}}$, respectively, and the outer disc ionisation was $\xi = 30\,\mathrm{ergs{\cdot}cm\,s^{-1}}$. The boundary radius was set to $r_{\mathrm{boundary}} = 4\,r_{\mathrm{g}}$. The innermost radius coincides with the marginally stable orbit, and the outer radius was set to $400\,r_{\mathrm{g}}$. The spin value was chosen to be $a = 0.94$, i.e. $r_{\mathrm{ms}} \approx 2\,r_{\mathrm{g}}$. The inclination angle was chosen to 30 deg which is a typical value for the inclination of Seyfert 1 galaxies. The primary power-law radiation photon index and normalisation were set to $\Gamma = 1.9$ and $K_\Gamma = 10^{-3}$. We assumed isotropic irradiation, i.e. disc-sandwiching corona scenario. The standard value,

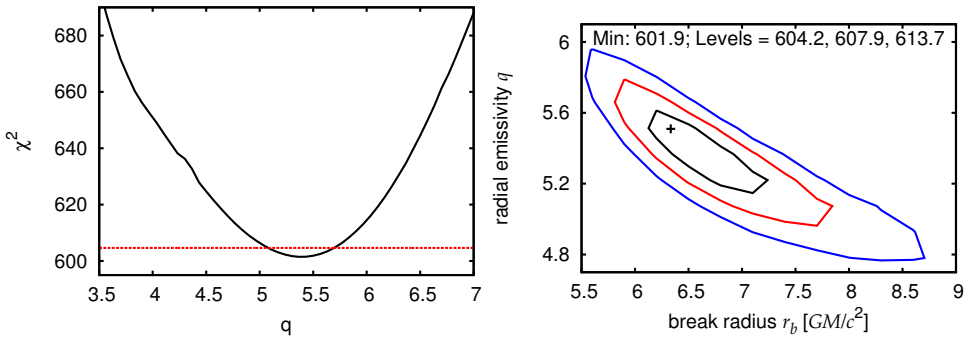

Figure 3. Left: Dependence of the fit-goodness on the radial emissivity parameter of the single reflection model. **Right:** The contour graph between the radial emissivity and the break radius. The default data were created by the two-reflection model with the inclination $i = 30$ deg, the break radius $r_{\mathrm{b,def}} = 4\,r_{\mathrm{g}}$, and the ionizations $\xi_{\mathrm{in}} = 130$ and $\xi_{\mathrm{out}} = 30$.

Table 2. Resulting parameter values of the single reflection model applied to the data simulated by a "two-reflection" model.

ξ_{in} / ξ_{out} (def.)	q	r_{b}	ξ	χ^2/ν
50 / 30	$4.04^{+0.76}_{-0.48}$	$6.1^{+1.7}_{-1.2}$	28^{+11}_{-6}	544/604
80 / 30	$4.70^{+0.73}_{-0.87}$	$6.6^{+0.8}_{-0.9}$	25^{+8}_{-3}	542/604
100 / 30	$4.88^{+0.36}_{-0.69}$	$6.1^{+1.2}_{-0.6}$	23^{+3}_{-2}	548/604
130 / 30	$4.93^{+0.20}_{-0.26}$	$7.1^{+0.7}_{-0.6}$	24^{+3}_{-2}	569/604
150 / 30	$5.51^{+0.19}_{-0.43}$	$6.3^{+0.8}_{-0.4}$	21^{+1}_{-1}	602/604
200 / 30	$4.95^{+0.45}_{-0.15}$	$8.3^{+0.8}_{-1.0}$	21^{+1}_{-5}	652/604

Table 3. Resulting parameter values of the single reflection model applied to the data simulated by a "complex" reflection model.

parameter	default value	fit value	error
photon index	1.9	2.10	0.05
power-law norm.	10^{-3}	2.55×10^{-3}	0.15×10^{-3}
spin	0.94	0.94	f
inclination [deg]	30	30	f
inner rad. emissivity	3	4.2	0.1
break radius [r_{g}]	–	35	20
ionisation [ergs·cm s^{-1}]	different	40	10
refl. norm.	10^{-5}	2×10^{-4}	0.5×10^{-4}
fit goodness	$\chi^2/\nu \approx 0.96$	$\chi^2/\nu \approx 1.13$	–

Note: the sign 'f' in the error column means that the values were frozen during the fitting procedure.

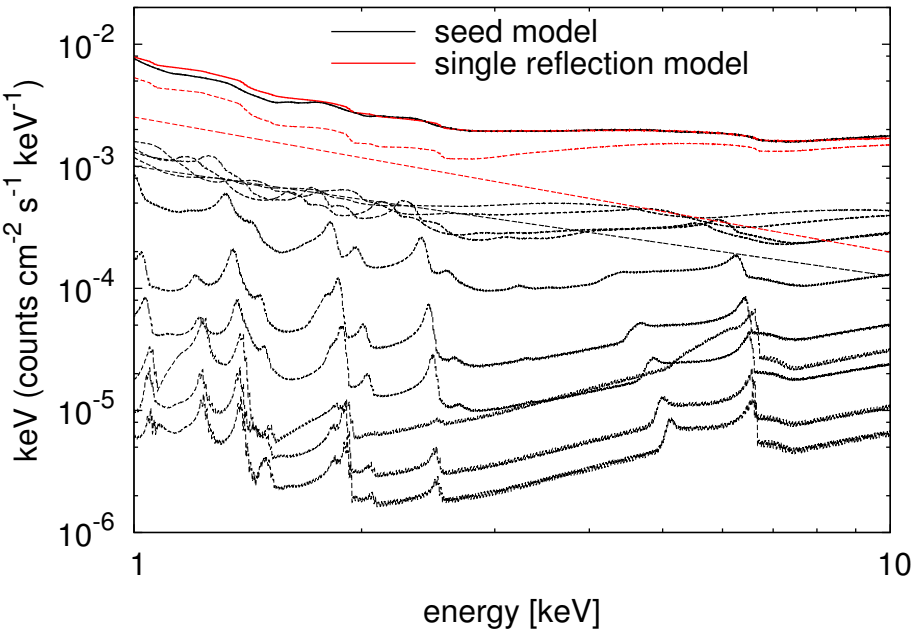

Figure 4. Comparison of the 'complex' and the 'single' ionisation reflection model. The solid lines show the total model fluxes while the dashed ones are their components. The straight dashed lines correspond to the power-law continua irradiating the disc. Black: the seed 'complex' reflection model and its components. The iron line around 6 keV may be used as a diagnostic of the individual components. The more smeared and red-shifted iron lines belong to the more ionised innermost parts of the disc. The cold reflection from the outer disc ($17–400\,r_{\rm g}$) is the one with the most blue-shifted peak, the fourth weakest component at 10 keV. Red: the best-fit single-ionisation reflection model. See the main text for more details.

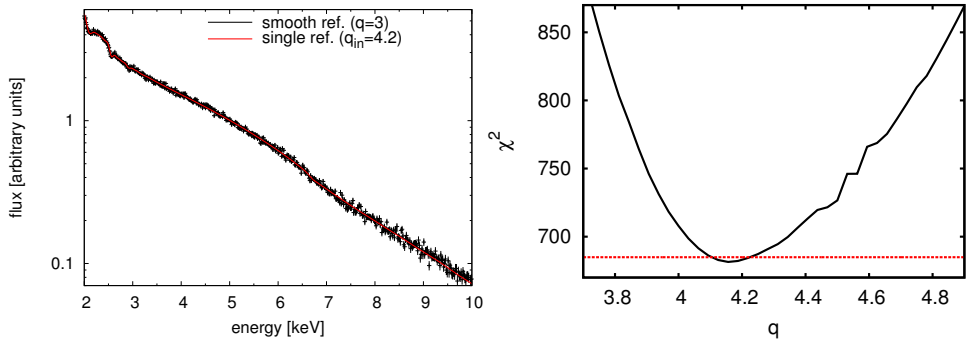

Figure 5. *Left:* The degeneracy between the radially-structured ionisation and the radial emissivity for the reflected radiation. Black: data generated with the radially decreasing ionisation, red: the best fit with a single ionisation but steeper radial emissivity. *Right:* Dependence of the fit goodness on the radial emissivity index for the single-ionisation reflection model.

$q = 3$, was adopted for the radial emissivity index. For the reflection components, we used solar iron abundances and normalisation $K_R = 10^{-5}$, fixed to the same value for each component.

We generated the data by this model in the same way as described in Section 2. Then we fit the data in the 2–10 keV energy range with a model consisting of only a power-law continuum and a single reflection component with a broken power-law radial emissivity. The photon index, the inner radial emissivity index, the break radius, the ionisation and the normalisations were the only parameters which were allowed to vary during the fitting procedure. The best-fit values and the errors are summarised in Table 2. A significant steepening of the radial emissivity occurs already for a relatively small ionisation gradient. The highest value of the radial emissivity index, $q \approx 5.5$, was found for $\xi_{\rm in} = 150$ ergs·cm s^{-1}. The dependence of the fit goodness and the contours between the radial emissivity and the break radius are shown in Fig. 3 for this case, and in the Appendix (Figs. 9–14) for the other parameters.

For larger values than $\xi_{\rm in} \approx 200$, the ionisation component becomes much more significant than the cold reflection, dominates in the total spectrum, and the interplay between the ionised and the cold component vanishes. This is due to the fact that the efficiency of the reflection from the ionised surface is much higher (Ross and Fabian, 2005). Table 2 also shows the goodness of the best fit. The resulting χ^2-values increase with the larger ionisation gradient in the simulated data. This suggests that the radially structured ionisation cannot be simply modelled in the 2–10 keV energy range by a single-ionisation component with the broken power-law radial emissivity and with the assumption of the existence of the outer disc ($r_{\rm out} = 400\, r_{\rm g}$) where the radial emissivity decreases as r^{-3}.

Rather surprising result is that the best-fit value of the single ionisation parameter has always a lower value than the default one for the outer-disc ionisation. Also, the value of the break radius of the radial emissivity is in all the fits higher than the value of the boundary radius used in the simulations.

5.2 Smooth decrease of ionisation

The previous analysis showed that ionisation gradient plays an important role in the total shape of the reflection spectra. Further, we considered a rather smooth radial decrease of the disc ionisation. We used 10 regions with decreasing ionisation: 200, 170, 140, 110, 80, 50, 30, 20, 15, 10 ergs·cm s^{-1}, with the boundaries at the radii: 3, 4, 5, 7, 9, 11, 13, 15, 17 $r_{\rm g}$, respectively. The other parameters were the same as before. We call this model as a "complex" reflection model, and it is plotted in the 1–10 keV energy range in Fig. 4.

The data were generated by this model in the same way as described in Section 2, and then fitted in the 2–10 keV energy range with a model consisting of only a power-law continuum and a single reflection component with a broken power-law radial emissivity. The photon index, the inner radial emissivity index, the break radius, the ionisation and the normalisations were the only parameters which were allowed to vary during the fitting procedure. The best-fit model is compared to the seed model in Fig. 4.

Figure 5 (left panel) shows how well the single-reflection model suits to the data in the 2–10 keV energy range. This clearly reveals the degeneracy between the radially-structured ionisation and the radial emissivity of the re-processed radiation smeared by the relativistic effects. The radial emissivity index is required to be significantly steeper in the single-

reflection model, $q \geq 4$, whereas with the standard value, $q = 3$, the fit gives high $\chi^2/\nu \approx 3.1$. See also the right panel of Fig. 5. The best-fit parameters are summarised in Table 3. In addition to the steepening of the radial emissivity, the photon index of the primary power-law was found to be significantly larger. It changed from the value $\Gamma = 1.9$ to $\Gamma = 2.1$. This softening of the primary power-law is due to the different slope of the ionised reflection continuum.

6 DISCUSSION

We addressed steep radial emissivities recently detected in the reflection components of the X-ray spectra of active galaxies and black-hole binaries. We investigated some possible explanations. To this end, we performed several simulations to reveal the degeneracies of the radial emissivity with other parameters and intrinsic assumptions of the relativistic reflection model.

6.1 Lamp-post scenario

The steep radial emissivity may be related to the properties of the disc-illuminating corona as suggested before by Wilms et al. (2001). The geometry of the emitting region certainly plays a significant role. A very centrally localised source at a low height above the black hole horizon would irradiate the disc mainly in its central region. The illumination in this area is greatly enhanced due to the gravitational light-bending effect (Miniutti and Fabian, 2004; Wilkins and Fabian, 2011, Dovčiak et al., in prep.).

To achieve steep radial emissivity, which is assumed to be proportional to the illumination, the source must be sufficiently close to the black hole. However, in this case the primary emission has to be extremely bright because only a small fraction would overcome the strong gravitational pull of the black hole and reach the observer (see Fig. 2 in Dovčiak et al., 2011). The importance of these effects drops quickly with the height. Already at heights $h \gtrsim 3\,r_{\rm g}$ the radial emissivity profile is similar to the simple power-law with the standard value ($q = 3$). For even larger heights, the irradiation profile is more complicated (see Fig. 3 and 4 in Dovčiak et al., 2011). It decreases steeply only very close to the black-hole horizon, then becomes rather flat ($q < 3$) still in the inner parts of the disc and finally reaches the standard value far from the centre.

Although this effect may steepen the radial emissivity significantly, a very large value, $q \approx 7$, as observed by Fabian et al. (2009); Wilkins and Fabian (2011) has not been reached in our calculations (Dovčiak et al., in prep.) even when the height was set very close to the black hole. We therefore proposed additional explanation.

6.2 Angular directionality

For the angular emissivity, the limb darkening law is frequently used. Several simulations, however, suggest that the directionality is opposite to limb darkening (see e.g. Różańska et al., 2011 and references therein). The emission angle in the innermost region of the disc is always very high due to the strong aberration. The flux contribution from this region is therefore underestimated by models with limb darkening if the angular emissivity is indeed different. This effect could lead to an approximately 20 % overestimation of the spin or the inner radial emissivity parameter. Svoboda et al. (2009) re-analysed the

XMM-Newton observation of MCG -6-30-15 and showed that the radial emissivity might be a more sensitive parameter to the angular directionality than the spin. This is especially true when the spin value itself is very high (close to one).

6.3 Radially structured ionisation

We also discussed the impact of the probable radial dependence of the disc surface ionisation. The disc illumination by corona is commonly assumed to be stronger in the innermost regions. Therefore, we simply assumed that the ionisation is higher at the innermost region as well, and decreases with the radius. We have not considered other aspects which affect the ionisation structure of the disc such as the density profile, vertical structure, and thermal processes (the last one especially relevant for the stellar-mass black hole binaries). With our simple assumption, we performed several tests with the simulated data using different initial values of the model parameters.

The broad iron-line profile is formed by two competing effects – the ionisation that shifts the rest energy of the line to higher values and the gravitational redshift with the opposite impact. The latter effect prevails sufficiently close to the black hole, and so the line is still shifted downwards from the rest neutral iron line energy in the more ionised central regions. The contribution to the reflection spectral component is higher from the more ionised part of the disc, which is located closer to the centre. Thus, ionisation contributes to the red wing of the broad relativistic line, as limb brightening and steep radial emissivity do. Consequently, when a simplified model with a single ionisation is used for fitting the data it may lead to an underestimation of the flux from the innermost regions.

In the presented analysis, we used an assumption of the fixed normalisations between the individual REFLIONX components. The ionisation parameter is defined there as $\xi = 4\pi F_{\rm inc}/n_{\rm H}$, where $F_{\rm inc}$ is the incident flux, and $n_{\rm H}$ is the hydrogen number density. This means that the higher ionisation parameter implies larger incident flux and consequently, also the more intense reflected flux. The mutual dependence between the irradiating flux and the ionisation parameter can be intuitively expected. However, a simple proportionality will have to be eventually replaced by a more complicated relation taking into account the actual solution of the radiation reprocessing of the incident flux in the disc medium as well as the effects of general relativity.

The contribution from the ionised reflection is thus larger for a given value of the normalisation. The higher radial emissivity parameter, q, found in the fitting by the single-reflection model is partly due to higher ionising incident flux and partly due to a different shape of the ionised reflection component. As a next step, we intend to fix the normalisation factors in a self-consistent way with the assumed incident flux that decreases smoothly with the radius. We also plan to take the radial dependence of the density into account in the forthcoming analysis.

7 CONCLUSIONS

The very steep radial emissivity of the disc reflection, which has been recently detected in the X-ray spectra of active galactic nuclei and black hole binaries, may be explained by geometrical properties of the disc-illuminating corona, by radially structured ionisation

and/or by use of an improper model assumption about the angular directionality. The first puts rather extreme requirements on the corona. It needs to be very bright and occur at a very low height above the black hole. We realised that the radial decrease of the disc ionisation may account for the radial-emissivity steepness equally well as the assumption of the centrally localised corona. If the ionisation decreases with growing distance from the black hole, the contribution from the innermost region is enhanced due to the larger reflection efficiency. The reported very high values for the radial emissivity in several sources, like $q \approx 7$, suggest that all of the discussed effects may take part together. Due to degeneracy it is difficult to distinguish among these effects from the spectral analysis of real data, and therefore, more theoretical attempts to constrain the disc-corona interactions are desirable. Development of a model with the self-consistent calculations of the disc surface ionisation that would depend on the irradiation intensity should be the next step in this research.

ACKNOWLEDGEMENTS

The present work was supported by the Czech Grant GAČR 14-20970P and the EU 7th Framework Programme No. 312789 "StrongGravity". JS thanks Prashin Jethwa for useful comments and also some language corrections.

REFERENCES

Arnaud, K. A. (1996), XSPEC: The First Ten Years, in G. H. Jacoby and J. Barnes, editors, *Astronomical Data Analysis Software and Systems V*, volume 101 of *Astronomical Society of the Pacific Conference Series*, p. 17.

Ballantyne, D. R., McDuffie, J. R. and Rusin, J. S. (2011), A Correlation between the Ionization State of the Inner Accretion Disk and the Eddington Ratio of Active Galactic Nuclei, *Astrophys. J.*, **734**, 112.

Ballantyne, D. R., Ross, R. R. and Fabian, A. C. (2001), X-ray reflection by photoionized accretion discs, *Monthly Notices Roy. Astronom. Soc.*, **327**, pp. 10–22, arXiv: `astro-ph/0102040`.

Beckwith, K. and Done, C. (2004), Iron line profiles in strong gravity, *Monthly Notices Roy. Astronom. Soc.*, **352**, pp. 353–362, arXiv: `astro-ph/0402199`.

Bhayani, S. and Nandra, K. (2011), On the apparent absence of broad iron lines in Seyfert galaxies, *Monthly Notices Roy. Astronom. Soc.*, **416**, pp. 629–636.

Blandford, R. D. and Znajek, R. L. (1977), Electromagnetic extraction of energy from Kerr black holes, *Monthly Notices Roy. Astronom. Soc.*, **179**, pp. 433–456.

Brenneman, L. W., Elvis, M., Krongold, Y., Liu, Y. and Mathur, S. (2012), NGC 5548: Lack of a Broad Fe Kα Line and Constraints on the Location of the Hard X-Ray Source, *Astrophys. J.*, **744**, 13, arXiv: `1109.4651`.

Brenneman, L. W. and Reynolds, C. S. (2006), Constraining Black Hole Spin via X-Ray Spectroscopy, *Astrophys. J.*, **652**, pp. 1028–1043, arXiv: `astro-ph/0608502`.

Czerny, B. and Goosmann, R. (2004), Flare-induced fountains and buried flares in AGN, *Astronomy and Astrophysics*, **428**, pp. 353–363, arXiv: `astro-ph/0408472`.

Dauser, T., Svoboda, J., Schartel, N., Wilms, J., Dovčiak, M., Ehle, M., Karas, V., Santos-Lleó, M. and Marshall, H. L. (2012), Spectral analysis of 1h 0707-495 with xmm-newton, *Monthly Notices Roy. Astronom. Soc.*, **422**(3), pp. 1914–1921.

Dovciak, M. (2004), *Radiation of Accretion Discs in Strong Gravity*, Ph.D. thesis, PhD Thesis, 2004, arXiv: arXiv:astro-ph/0411605.

Dovčiak, M., Karas, V. and Yaqoob, T. (2004), An Extended Scheme for Fitting X-Ray Data with Accretion Disk Spectra in the Strong Gravity Regime, *Astrophys. J. Suppl.*, **153**, pp. 205–221, arXiv: astro-ph/0403541.

Dovčiak, M., Muleri, F., Goosmann, R. W., Karas, V. and Matt, G. (2011), Light-bending Scenario for Accreting Black Holes in X-ray Polarimetry, *Astrophys. J.*, **731**, 75, arXiv: 1102.4247.

Dumont, A.-M., Abrassart, A. and Collin, S. (2000), A code for optically thick and hot photoionized media, *Astronomy and Astrophysics*, **357**, pp. 823–838, arXiv: astro-ph/0003220.

Fabian, A. C., Vaughan, S., Nandra, K., Iwasawa, K., Ballantyne, D. R., Lee, J. C., De Rosa, A., Turner, A. and Young, A. J. (2002), A long hard look at MCG-6-30-15 with XMM-Newton, *Monthly Notices Roy. Astronom. Soc.*, **335**, pp. L1–L5, arXiv: astro-ph/0206095.

Fabian, A. C., Zoghbi, A., Ross, R. R., Uttley, P., Gallo, L. C., Brandt, W. N., Blustin, A. J., Boller, T., Caballero-Garcia, M. D., Larsson, J., Miller, J. M., Miniutti, G., Ponti, G., Reis, R. C., Reynolds, C. S., Tanaka, Y. and Young, A. J. (2009), Broad line emission from iron K- and L-shell transitions in the active galaxy 1H0707-495, *Nature*, **459**, pp. 540–542.

George, I. M. and Fabian, A. C. (1991), X-ray reflection from cold matter in active galactic nuclei and X-ray binaries, *Monthly Notices Roy. Astronom. Soc.*, **249**, pp. 352–367.

Ghisellini, G., Haardt, F. and Matt, G. (1994), The Contribution of the Obscuring Torus to the X-Ray Spectrum of Seyfert Galaxies – a Test for the Unification Model, *Monthly Notices Roy. Astronom. Soc.*, **267**, p. 743, arXiv: astro-ph/9401044.

Goosmann, R. W., Czerny, B., Mouchet, M., Karas, V., Dovčiak, M., Ponti, G. and Różańska, A. (2006), Magnetic flares in Active Galactic Nuclei: modeling the iron Kα line, *Astronomische Nachrichten*, **327**, pp. 977–980, arXiv: astro-ph/0611020.

Goosmann, R. W., Mouchet, M., Czerny, B., Dovčiak, M., Karas, V., Różańska, A. and Dumont, A.-M. (2007), Iron lines from transient and persisting hot spots on AGN accretion disks, *Astronomy and Astrophysics*, **475**, pp. 155–168, arXiv: 0709.1356.

Haardt, F. (1993), Anisotropic Comptonization in thermal plasmas – Spectral distribution in plane-parallel geometry, *Astrophys. J.*, **413**, pp. 680–693.

Haardt, F. and Maraschi, L. (1991), A two-phase model for the X-ray emission from Seyfert galaxies, *Astronomy and Astrophysics Lett.*, **380**, pp. L51–L54.

Kawanaka, N., Mineshige, S. and Iwasawa, K. (2005), Iron Fluorescent Line Emission from Black Hole Accretion Disks with Magnetic Reconnection-heated Corona, *Astrophys. J.*, **635**, pp. 167–172, arXiv: astro-ph/0508507.

Laor, A. (1991), Line profiles from a disk around a rotating black hole, *Astrophys. J.*, **376**, pp. 90–94.

Martocchia, A., Karas, V. and Matt, G. (2000), Effects of Kerr space-time on spectral features from X-ray illuminated accretion discs, *Monthly Notices Roy. Astronom. Soc.*, **312**, pp. 817–826, arXiv: astro-ph/9910562.

Martocchia, A., Matt, G. and Karas, V. (2002), On the origin of the broad, relativistic iron line of MCG-6-30-15 observed by XMM-Newton, *Astronomy and Astrophysics*, **383**, pp. L23–L26.

Matt, G., Fabian, A. C. and Ross, R. R. (1993), Iron K-alpha lines from X-ray photoionized accretion discs, *Monthly Notices Roy. Astronom. Soc.*, **262**, pp. 179–186.

Matt, G., Perola, G. C. and Piro, L. (1991), The iron line and high energy bump as X-ray signatures of cold matter in Seyfert 1 galaxies, *Astronomy and Astrophysics*, **247**, pp. 25–34.

Merloni, A., Heinz, S. and di Matteo, T. (2003), A Fundamental Plane of black hole activity, *Monthly Notices Roy. Astronom. Soc.*, **345**, pp. 1057–1076, arXiv: astro-ph/0305261.

Miller, J. M. (2007), Relativistic X-Ray Lines from the Inner Accretion Disks Around Black Holes, *Annual Review of Astronomy & Astrophysics*, **45**, pp. 441–479, arXiv: 0705.0540.

Miniutti, G. and Fabian, A. C. (2004), A light bending model for the X-ray temporal and spectral properties of accreting black holes, *Monthly Notices Roy. Astronom. Soc.*, **349**, pp. 1435–1448, arXiv: astro-ph/0309064.

Miniutti, G., Fabian, A. C., Anabuki, N., Crummy, J., Fukazawa, Y., Gallo, L., Haba, Y., Hayashida, K., Holt, S., Kunieda, H., Larsson, J., Markowitz, A., Matsumoto, C., Ohno, M., Reeves, J. N., Takahashi, T., Tanaka, Y., Terashima, Y., Torii, K., Ueda, Y., Ushio, M., Watanabe, S., Yamauchi, M. and Yaqoob, T. (2007), Suzaku Observations of the Hard X-Ray Variability of MCG -6-30-15: the Effects of Strong Gravity around a Kerr Black Hole, *Publications of the Astronomical Society of Japan*, **59**, pp. 315–325, arXiv: astro-ph/0609521.

Miniutti, G., Fabian, A. C., Goyder, R. and Lasenby, A. N. (2003), The lack of variability of the iron line in MCG-6-30-15: general relativistic effects, *Monthly Notices Roy. Astronom. Soc.*, **344**, pp. L22–L26, arXiv: astro-ph/0307163.

Nandra, K. (2011), ATHENA: The Advanced Telescope for High Energy Astrophysics, in J.-U. Ness and M. Ehle, editors, *The X-ray Universe 2011*, p. 22.

Nandra, K., O'Neill, P. M., George, I. M. and Reeves, J. N. (2007), An XMM-Newton survey of broad iron lines in Seyfert galaxies, *Monthly Notices Roy. Astronom. Soc.*, **382**, pp. 194–228, arXiv: 0708.1305.

Nayakshin, S. and Kallman, T. R. (2001), Accretion Disk Models and Their X-Ray Reflection Signatures. I. Local Spectra, *Astrophys. J.*, **546**, pp. 406–418, arXiv: astro-ph/0005597.

Novikov, I. D. and Thorne, K. S. (1973), Astrophysics of black holes., in C. Dewitt and B. S. Dewitt, editors, *Black Holes (Les Astres Occlus)*, pp. 343–450.

Penna, R. F., McKinney, J. C., Narayan, R., Tchekhovskoy, A., Shafee, R. and McClintock, J. E. (2010), Simulations of magnetized discs around black holes: effects of black hole spin, disc thickness and magnetic field geometry, *Monthly Notices Roy. Astronom. Soc.*, **408**, pp. 752–782, arXiv: 1003.0966.

Ponti, G., Gallo, L. C., Fabian, A. C., Miniutti, G., Zoghbi, A., Uttley, P., Ross, R. R., Vasudevan, R. V., Tanaka, Y. and Brandt, W. N. (2010), Relativistic disc reflection in the extreme NLS1 IRAS13224-3809, *Monthly Notices Roy. Astronom. Soc.*, **406**, pp. 2591–2604, arXiv: 0911.1003.

Reynolds, C. S., Brenneman, L. W., Wilms, J. and Kaiser, M. E. (2004), Iron line spectroscopy of NGC 4593 with XMM-Newton: where is the black hole accretion disc?, *Monthly Notices Roy. Astronom. Soc.*, **352**, pp. 205–210, arXiv: astro-ph/0404187.

Reynolds, C. S. and Nowak, M. A. (2003), Fluorescent iron lines as a probe of astrophysical black hole systems, *Physics Reports*, **377**, pp. 389–466, arXiv: astro-ph/0212065.

Ross, R. R. and Fabian, A. C. (2005), A comprehensive range of X-ray ionized-reflection models, *Monthly Notices Roy. Astronom. Soc.*, **358**, pp. 211–216, arXiv: astro-ph/0501116.

Różańska, A., Dumont, A.-M., Czerny, B. and Collin, S. (2002), The structure and radiation spectra of illuminated accretion discs in active galactic nuclei - I. Moderate illumination, *Monthly Notices Roy. Astronom. Soc.*, **332**, pp. 799–813, arXiv: astro-ph/0202069.

Różańska, A., Madej, J., Konorski, P. and SaĻowski, A. (2011), Iron lines in model disk spectra of Galactic black hole binaries, *Astronomy and Astrophysics*, **527**, A47, arXiv: 1011.2061.

Shakura, N. I. and Sunyaev, R. A. (1973), Black holes in binary systems. Observational appearance., *Astronomy and Astrophysics*, **24**, pp. 337–355.

Svoboda, J., Dovčiak, M., Goosmann, R. and Karas, V. (2009), Role of emission angular directionality in spin determination of accreting black holes with a broad iron line, *Astronomy and Astrophysics*, **507**, pp. 1–17, arXiv: 0908.2387.

Svoboda, J., Guainazzi, M. and Karas, V. (2010), Warm absorber and truncated accretion disc in IRAS 05078+1626, *Astronomy and Astrophysics*, **512**, A62, arXiv: 0912.5165.

Vaughan, S. and Fabian, A. C. (2004), A long hard look at MCG-6-30-15 with XMM-Newton- II. Detailed EPIC analysis and modelling, *Monthly Notices Roy. Astronom. Soc.*, **348**, pp. 1415–1438, arXiv: astro-ph/0311473.

Wilkins, D. R. and Fabian, A. C. (2011), Determination of the X-ray reflection emissivity profile of 1H 0707-495, *Monthly Notices Roy. Astronom. Soc.*, **414**, pp. 1269–1277, arXiv: 1102.0433.

Wilms, J., Reynolds, C. S., Begelman, M. C., Reeves, J., Molendi, S., Staubert, R. and Kendziorra, E. (2001), XMM-EPIC observation of MCG-6-30-15: direct evidence for the extraction of energy from a spinning black hole?, *Monthly Notices Roy. Astronom. Soc.*, **328**, pp. L27–L31, arXiv: astro-ph/0110520.

Zhou, X. L., Zhao, Y. H. and Soria, R. (2011), Ionization structure and Fe Kα energy for irradiated accretion discs, *Monthly Notices Roy. Astronom. Soc.*, **413**, pp. L61–L65, arXiv: 1102.3327.

Zoghbi, A., Fabian, A. C., Uttley, P., Miniutti, G., Gallo, L. C., Reynolds, C. S., Miller, J. M. and Ponti, G. (2010), Broad iron L line and X-ray reverberation in 1H0707-495, *Monthly Notices Roy. Astronom. Soc.*, **401**, pp. 2419–2432, arXiv: 0910.0367.

Zycki, P. T. and Czerny, B. (1994), The Iron K-Alpha Line from a Partially Ionized Reflecting Medium in an Active Galactic Nucleus, *Monthly Notices Roy. Astronom. Soc.*, **266**, p. 653.

APPENDIX

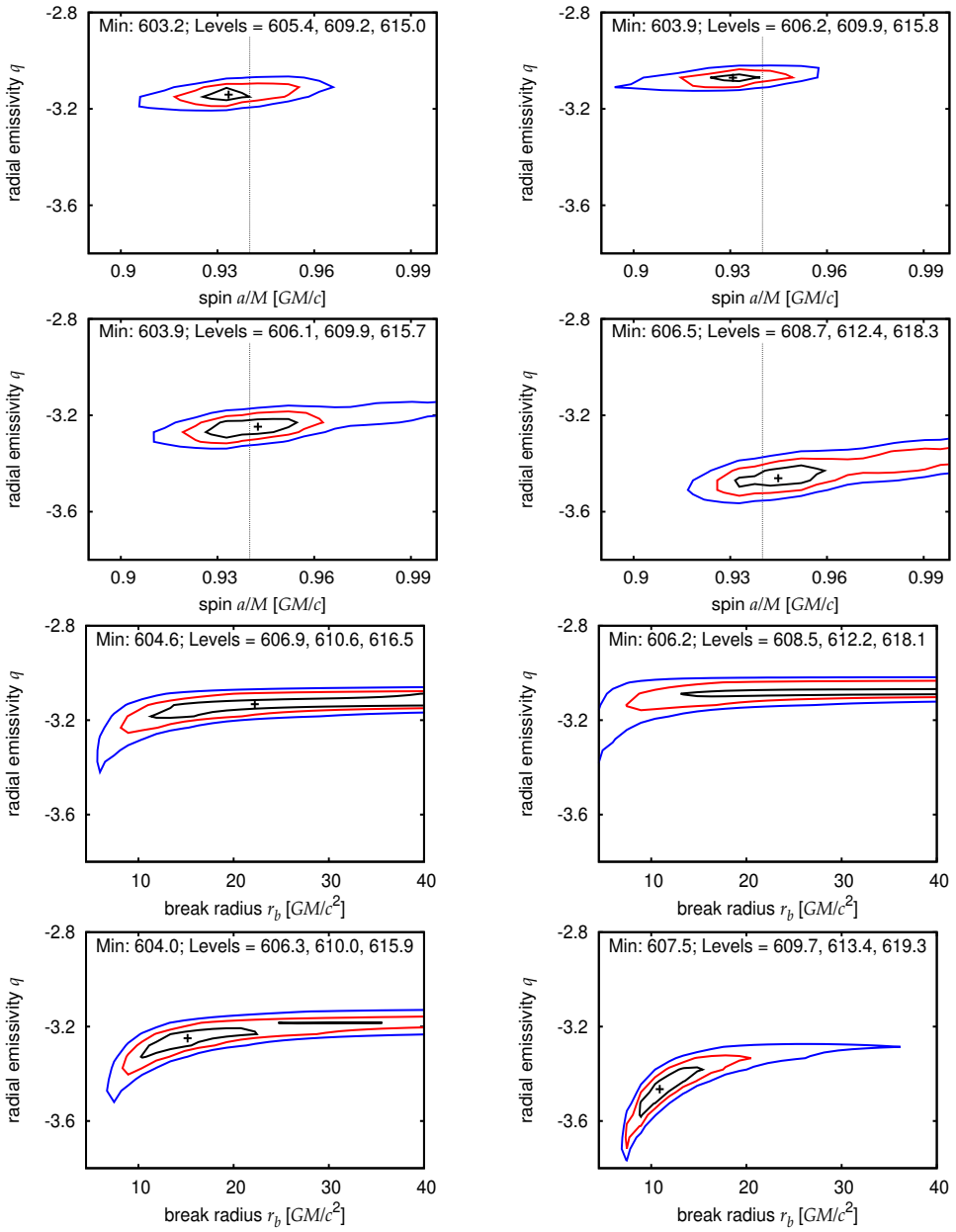

Figure 6. The same as in Fig. 1 and 2 but for the height $h = 3\,r_{\rm g}$.

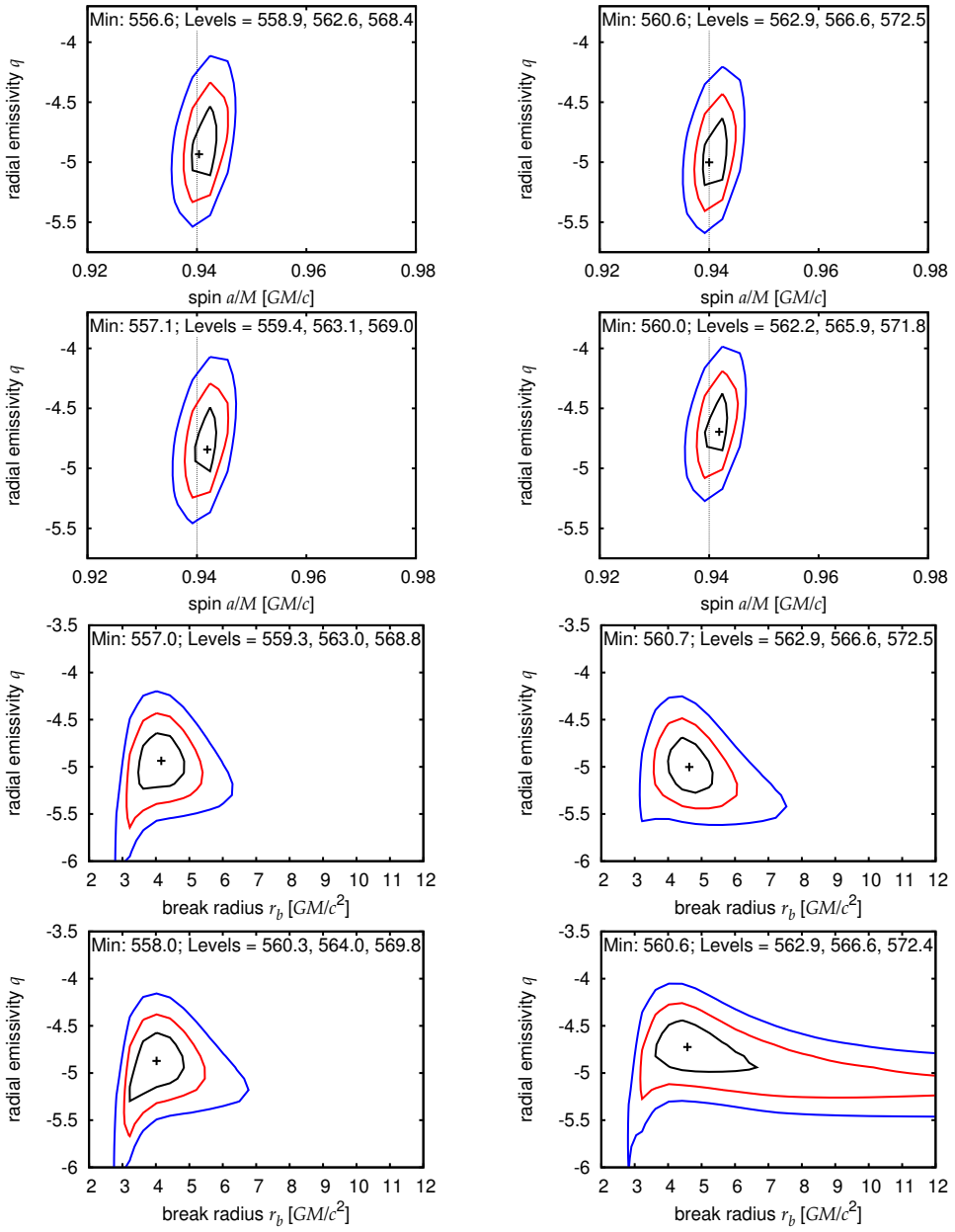

Figure 7. The same as in Fig. 1 and 2 ($h = 1.5\,r_{\rm g}$) but for inclination 70 deg.

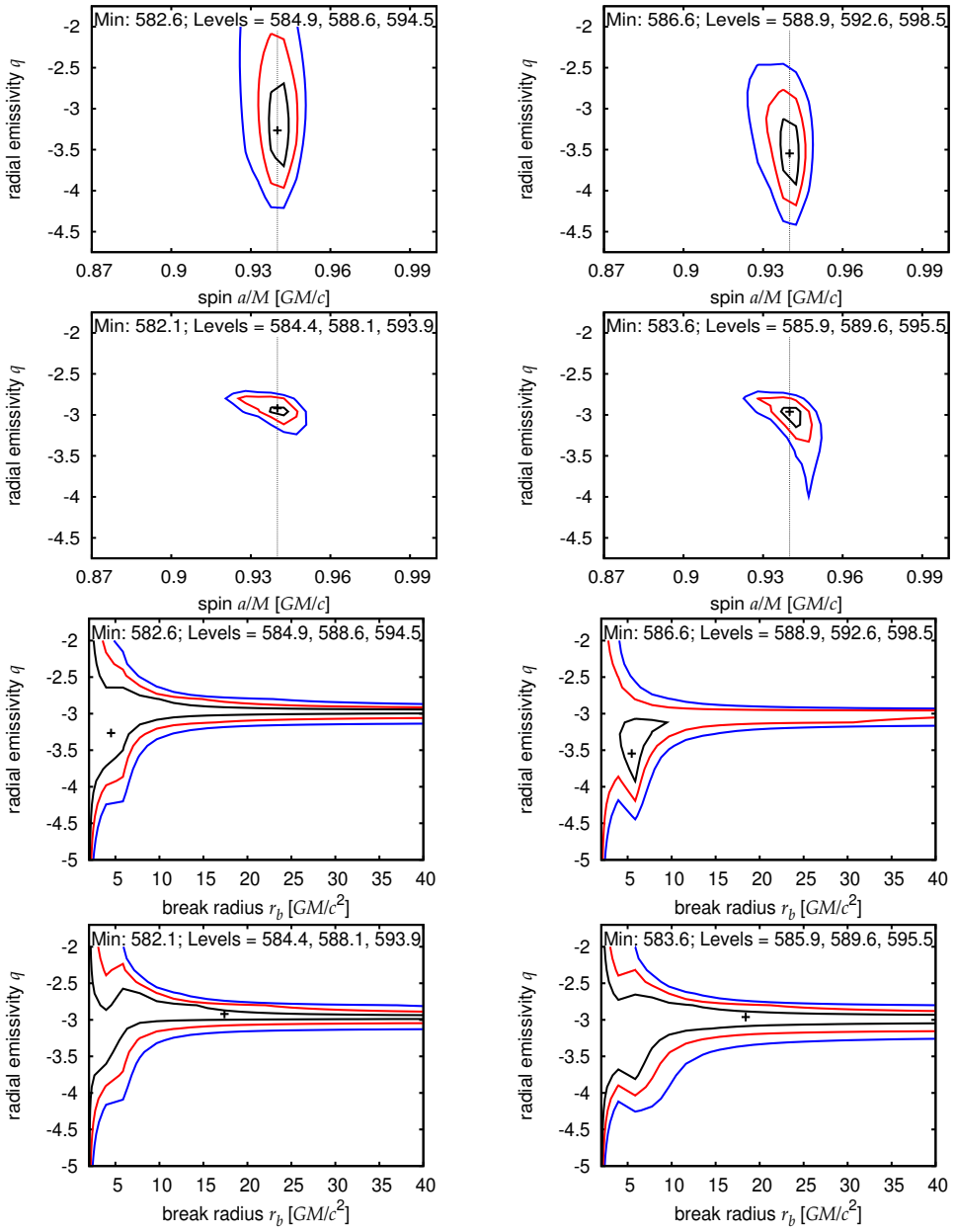

Figure 8. The same as in Fig. 6 ($h = 3\,r_{\rm g}$) but for inclination 70 deg.

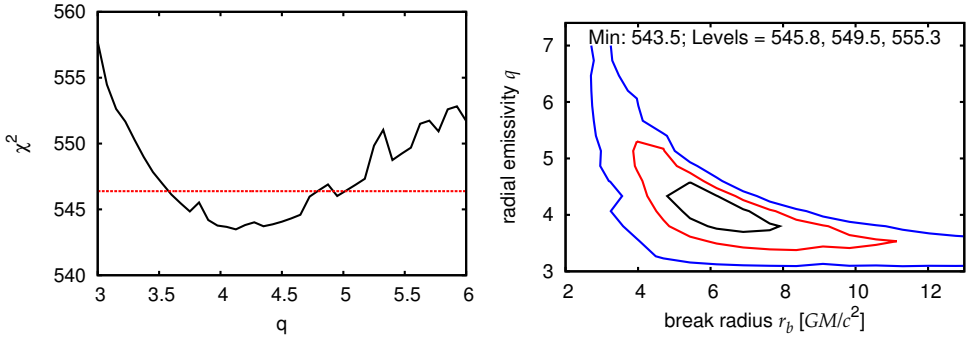

Figure 9. The same as in Fig. 3 but for $\xi_{\rm in} = 50$ and $\xi_{\rm out} = 30$.

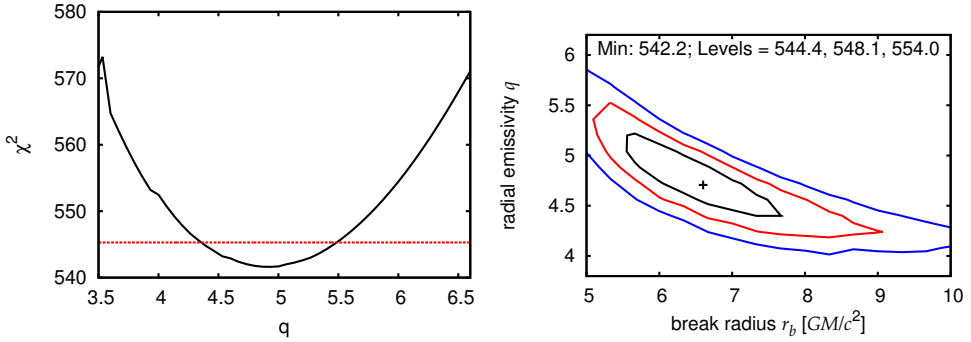

Figure 10. The same as in Fig. 3 but for $\xi_{\rm in} = 80$ and $\xi_{\rm out} = 30$.

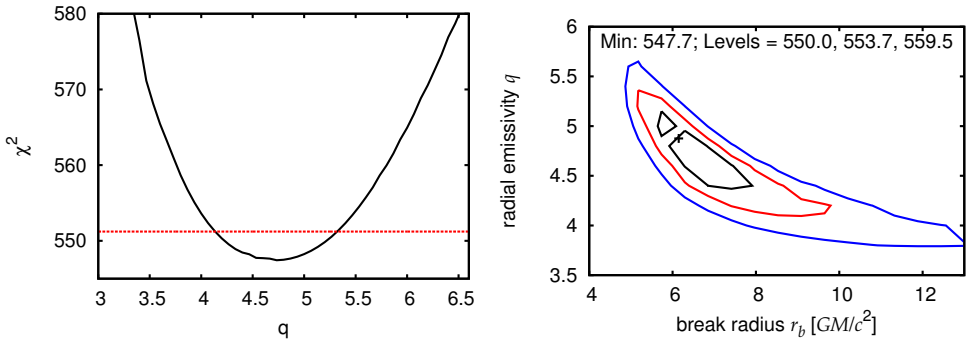

Figure 11. The same as in Fig. 3 but for $\xi_{\rm in} = 100$ and $\xi_{\rm out} = 30$.

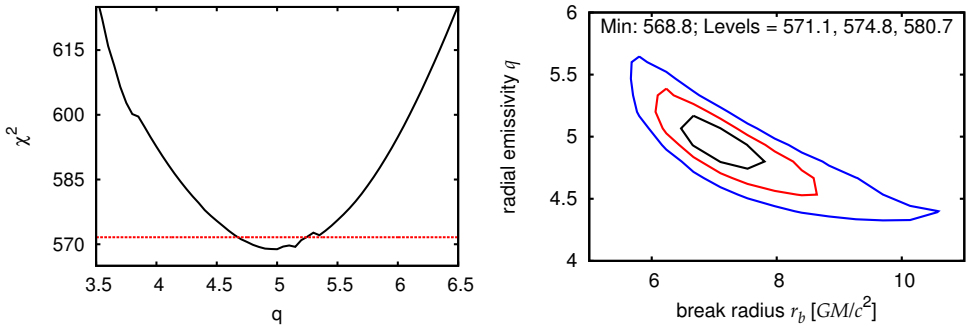

Figure 12. The same as in Fig. 3 but for $\xi_{\rm in} = 130$ and $\xi_{\rm out} = 30$.

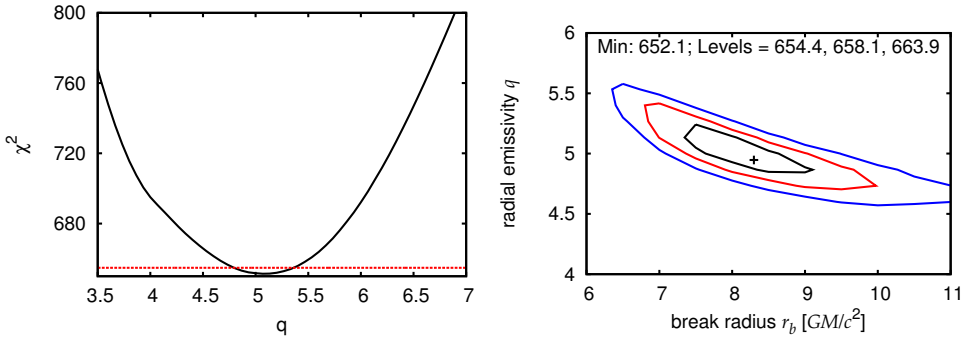

Figure 13. The same as in Fig. 3 but for $\xi_{\rm in} = 200$ and $\xi_{\rm out} = 30$.

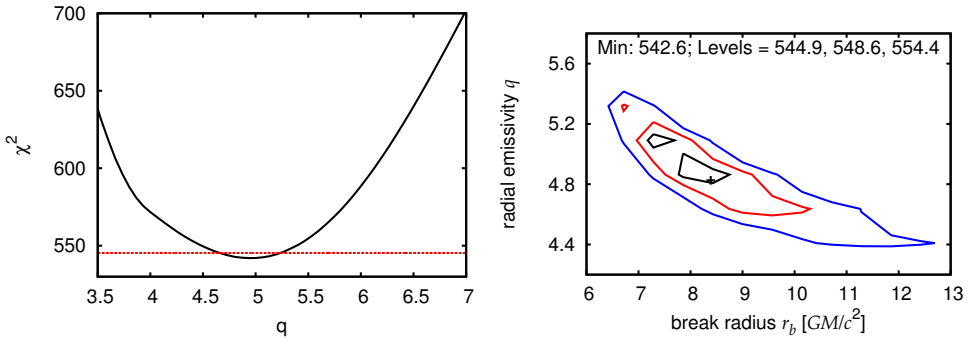

Figure 14. The same as in Fig. 13 but for spin $a = 0.99$.